Chapter 4

Interaction of a tightly focused radially polarized beam with a nanoparticle

This chapter focuses on influence of the polarization state of a tightly focused beam, on the plasmonic response of nanoparticles and intensity enhancement in the near-field. We developed the Mie Scattering Algorithm for a monometallic and a core-shell nanoparticle illuminated by a tightly focused radially polarized on a MATLAB platform. Average intensity enhancement on the surface of a plasmon-assisted nanoparticle is observed in different dielectric media air, BK7 (glass), and silicon. A detailed comparison is also made for intensity enhancement observed in near-field for three different illuminations: plane wave, tightly focused linearly polarized, and tightly focused radially polarized beam.

4.1 Introduction: Radially Polarized Tightly Focused Beams

The polarization state in the pupil before focusing influences the focal spot and its interaction with the matter [162-165]. An asymmetric deformation of the focal spot is observed in the case of a tightly focused linearly polarized beam. In contrast, this deformation is removed by tuning the polarization structure of the light source such as in radially or circularly polarized incident beam. Subsequent research revealed that a sharper focal spot is obtained for a radially polarized incident beam in comparison to the Airy disc of a low NA focusing system. A tightly focused radially polarized beam can produce strong longitudinal electric fields which also spurred their expanded adoption [70]. This characteristic has found uses in numerous applications including optical trapping, laser cutting, and improved resolution in imaging, and mapping orientation of single molecules [166-170].

A tightly focused radially polarized beam offers more opportunities while tuning the near and far-field system. The beam profile gets modified in the focal region according to the incident beam polarization state [171-175]. This affects the scattering behavior and the intensity enhancement in the near-field. Experimental studies showing applications based on the plasmonic properties of nanoparticles have also been using radially polarized tightly focused beams [102, 119, 176-178].

Radial polarization combines different linear polarizations whose orientations are axially distributed along the optical axis. Different components of the electric field of a tightly focused radially polarized beam for a focusing system with convergence angle $\boldsymbol{\alpha = 60}°$ at the focal plane are presented in Fig. 4.1. We simulated these results for wavelength $\boldsymbol{\lambda = 645\ nm}$. For a tightly focused radially polarized beam, a stronger z-component of the electric field is observed in the focal region.

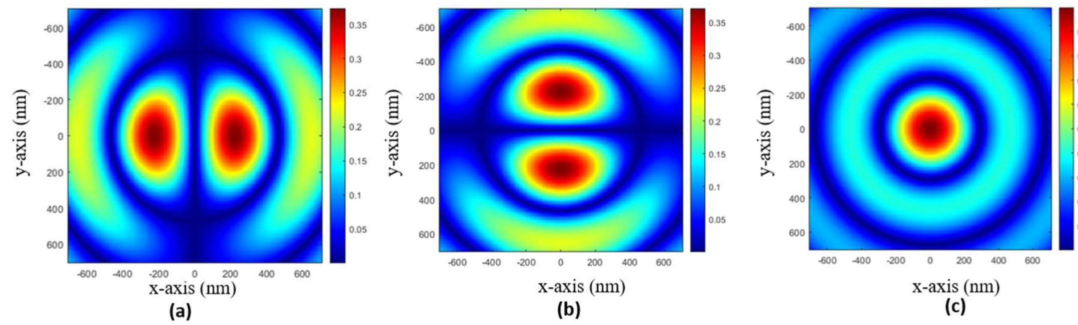

Fig. 4.1 Electric field components of a tightly focused radially polarized beam at the focal plane (a) $\boldsymbol{E_x(x,y)}$, (b) $\boldsymbol{E_y(x,y)}$, and (c) $\boldsymbol{E_z(x,y)}$. The results are normalized with the maximum value of the total absolute value of the electric field.

As discussed in **Section 3.1 (Chapter 3)**, the complex EM field distribution of a tightly focused beam with an arbitrary polarization, using Richard and Wolf's formalism, at the focal plane is expressed as 137, 144, 145]

$$\boldsymbol{E}(\vec{r_p}) = -\frac{ie^{ikf}}{\lambda}\int_0^{2\pi}\int_0^{\alpha} E_0(\theta,\phi)\,A(\theta)\,\mathcal{P}(\theta,\phi)\exp\left(i\vec{k}.\vec{r_p}\right) sin\theta d\theta d\phi, \qquad (4.1)$$

In the case of a uniform polarization, the strength of x and y-polarized incident beams is independent of the angular coordinates as in the case of a linear or circular polarization. On the other hand, in a non-uniform polarization case such as radial or azimuthal polarization the strength factors depend on the coordinate [99, 178]. Therefore, the strength factors for an incident radial polarization are $\boldsymbol{\mathcal{P}_x(\theta,\phi) = cos\phi}$, and $\boldsymbol{\mathcal{P}_y(\theta,\phi) = sin\phi}$, and the polarization distribution (Eq. (3.4), **Chapter 3**) for an incident radially polarized beam is expressed as [160, 161]

$$\mathcal{P}(\theta,\phi) = \begin{bmatrix} cos\theta\ cos\phi \\ cos\theta\ sin\phi \\ -sin\theta \end{bmatrix} \qquad (4.2)$$

Based on the polarization state of the incident beam i.e. radial, the electric field components of a tightly focused radially polarized beam near the focus are written as [165]

$$E_x(v, u, \phi_P) = K[iI_1\, cos(\phi_P)] \tag{4.3}$$

$$E_y(v, u, \phi_P) = K[iI_1\, sin(\phi_P)] \tag{4.4}$$

$$E_z(v, u, \phi_P) = -I_0 \tag{4.5}$$

where $K = -\left(\frac{ik}{2}\right) f exp(ikf) E_0$,

$$I_0(v, u) = \int_0^\alpha A(\theta)\, sin^2(\theta) J_0 \left[\frac{v}{sin\, \alpha} sin\, \theta\right] exp\left[i \frac{u}{sin^2\alpha} cos(\theta)\right] d\theta \tag{4.6}$$

$$I_1(v, u) = \int_0^\alpha A(\theta)\, sin(\theta) cos(\theta) J_1 \left[\frac{v}{sin\, \alpha} sin\, \theta\right] exp\left[i \frac{u}{sin^2\alpha} cos(\theta)\right] d\theta \tag{4.7}$$

On converting field distribution in spherical polar coordinates by replacing the Cartesian coordinate unit vectors, the electric field of a tightly focused radially polarized plane wave right after passing the lens is given by

$$\boldsymbol{E}_i(\theta) = E_0\, A(\theta)\, \widehat{e_\theta} \tag{4.8}$$

where, E_0 is the scalar amplitude of a plane wave, and $A(\theta) = \sqrt{cos(\theta)}$. The complex field derived using Richard and Wolf's formalism is now converted into multipole form using Mie theory to address the scattering process.

4.2 Mie scattering Algorithm for a tightly focused radially polarized beam

Since only θ component of field exists in the far field for a radially polarized beam in a tight focused condition, and the azimuthal number m vanishes for all multipoles, so $m = 0$ is considered [105]. Hence it is sufficient to express the field in terms of a single vector spherical harmonics N_{e0n}. By considering Mie theory and Richard and Wolf's formalism, the incident field for an incident tightly focused radially polarized beam is [65, 105, 137]

$$\boldsymbol{E}_i = \sum_{n=1}^{\infty} A_n \, \boldsymbol{N}_{e0n}^{(1)}, \tag{4.9}$$

and the corresponding expansion coefficient A_n is written as,

$$A_n = 2kf \, \frac{2n+1}{2n(n+1)i^n e^{-ik}} \int_0^{\alpha} |\boldsymbol{E}_i(\theta)| \, \frac{dP_n(\cos\theta)}{d\theta} \, sin\theta d\theta, \tag{4.10}$$

where $dP_n(\cos\theta)$ is the derivative of Legendre polynomial [105]. Since the incident field is determined now, and using Mie theory one can do further derivation for investigating the effect of interaction with a spherical nanoparticle. Thus, the respective scattered field is found to be

$$\boldsymbol{E}_s = \sum_{n=1}^{\infty} -a_n A_n \boldsymbol{N}_{e0n}^{(3)} \tag{4.11}$$

Here only one scattering coefficient a_n needs to be evaluated which has been discussed in **Section 2.1.1, and 2.1.2, Chapter 2** for a monometallic and a core-shell nanoparticle respectively.

4.3 Near field Intensity Enhancement

To further examine the impact of exotic beam structures at the focal plane and consider its influence on the scattering from the nanoparticle, we considered the scattering of a tightly focused radially polarized beam as shown in Fig. 4.2.

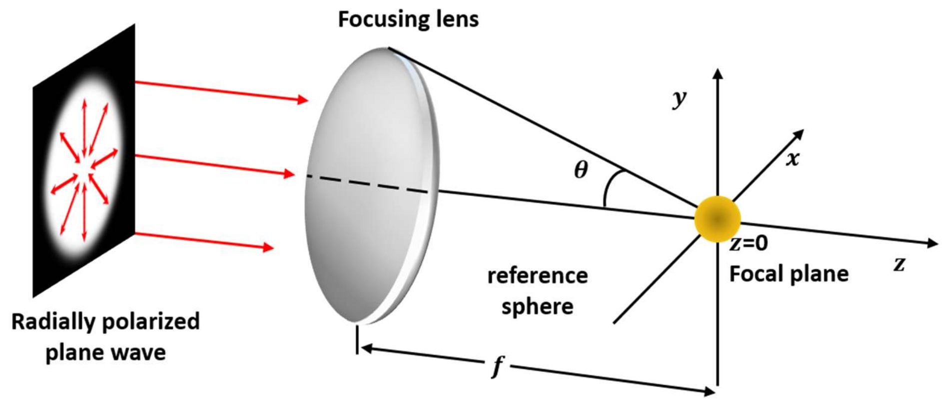

Fig. 4.2 Tightly focused radially polarized beam illuminating a nanoparticle kept at focus.

To study the plasmonic response of nanoparticles illuminated by an incident beam, an enhancement in near-field intensity is examined. The radial and tangential components of average intensity enhancement for a tightly focused radially polarized beam are derived by substituting Eqs. (4.9-4.11) in Eq. (1.9) (**Chapter 1**). The average radial and tangential intensity enhancement for a tightly focused radially polarized beam is written as [105],

$$K_r = \frac{9}{16(\rho)^4} \sum_n \frac{|A_n|^2}{|A_1|^2} \frac{4n^2(n+1)^2}{2n+1} [|a_n|^2 |\chi_n|^2 + |\psi_n|^2 + 2\, Re\{a_n^* \chi_n^*\} \psi_n], \qquad (4.12)$$

$$K_t = \frac{9}{16(\rho)^2} \sum_n \frac{|A_n|^2}{|A_1|^2} \frac{4n(n+1)}{2n+1} [|a_n|^2 \left|\chi_n^{'}\right|^2 + \left|\psi_n^{'}\right|^2 - 2\, Re\{a_n^* \chi_n^{'*}\} \psi_n^{'}]. \qquad (4.13)$$

Eq. (4.10) describes the expansion coefficients A_n, and $\rho = ka$ for a monometallic nanoparticle whereas for a core-shell nanoparticle $\rho = kb$ [65]. The scattering coefficient $a_n,\ b_n$ are taken from Eqs. (2.8-2.9), and Eqs. (2.10-2.13) (**Chapter 2**) for monometallic and core-shell nanoparticles respectively.

4.3 Results and Discussion

For investigating the scattering of a tightly focused radially polarized beam from a monometallic and core-shell nanoparticle, an algorithm is developed on MATLAB platform using Mie theory. Under different circumstances, the impact of tightly focused radially polarized beams on near-field intensity enhancement is examined. The angular semi aperture of a focusing lens is $\alpha = 60°$, and up to $n = 15$ multipoles are included for field expansion.

4.3.1 Monometallic nanoparticles

Scattering of an incident beam having a wavelength range 300 nm to 900 nm from an Au and an Ag nanoparticle of varying radius ranging from 1 nm to 100 nm are considered in two different dielectric media such as glass ($n_{glass} = 1.52$) and air ($n_{air} = 1.00$). Results of the average radial intensity enhancement for a tightly focused radially polarized beam with an Au nanoparticle in air and glass are shown in Fig. 4.3 (a), and Fig. 4.3 (b), respectively. A maximum intensity enhancement of 6.83 is observed at 548 nm wavelength in Fig. 4.3 (a) for an Au nanoparticle of radius 63 nm in air. Small-size Au nanoparticle shows a low enhancement factor, whereas the enhancement increases with an increase in the size of the particle. A maximum enhancement of 22.57 is observed at 570 nm wavelength for an Au nanoparticle of radius 31 nm in glass as shown in Fig. 4.3 (b).

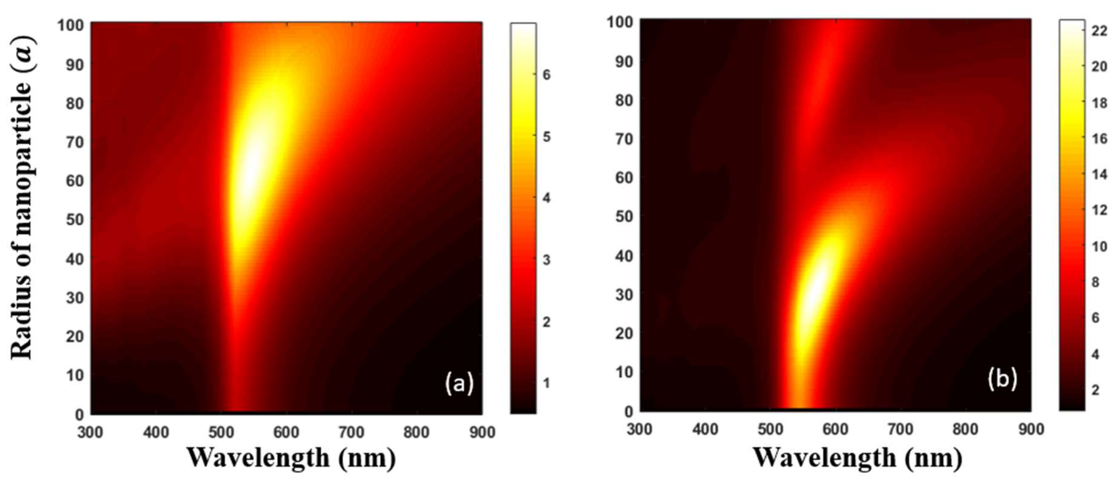

Fig. 4.3 Average radial intensity enhancement for an incident tightly focused radially polarized beam scattering from an Au nanoparticle in dielectric media (a) air, (b) glass.

The average radial intensity enhancement for an incident tightly focused radially polarized beam for an Ag nanoparticle in air and glass are presented in Fig. 4.4 (a) and Fig. 4.4 (b) respectively. Smaller size Ag nanoparticle shows a similar enhancement in all three cases for both dielectric media air and glass. Ag nanoparticle of radius 12 nm shows a maximum enhancement of 162.4 at 357 nm wavelength of the incident light in air, whereas Ag nanoparticle of radius 1 nm shows a maximum value 1380 at 403 nm wavelength in the glass.

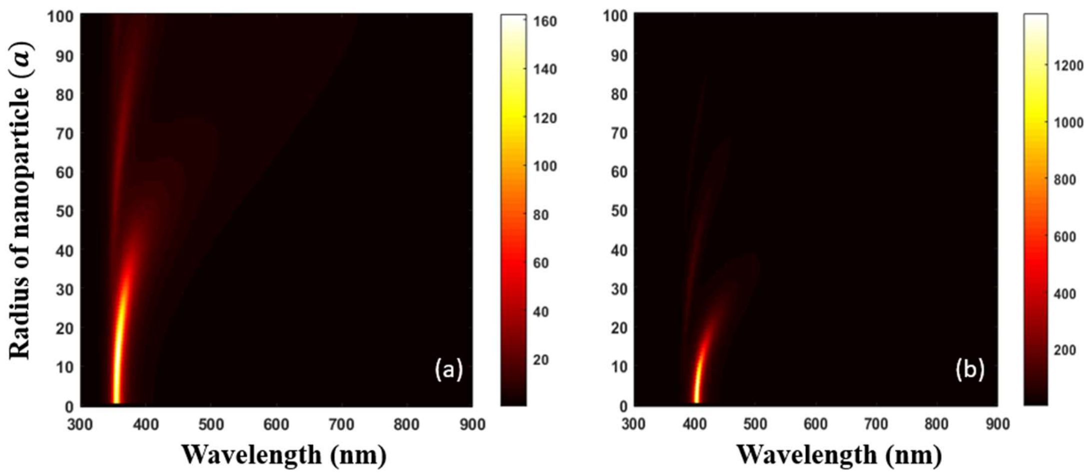

Fig. 4.4 Average radial intensity enhancement for an incident tightly focused radially polarized beam scattering from an Ag nanoparticle in dielectric media (a) air, (b) glass.

The maximum intensity enhancement factor for Au and Ag nanoparticles in dielectric media air and glass for a tightly focused radially polarized beam is tabulated in Table 4.1.

Table 4.1. Maximum Enhancement factor observed for Au and Ag nanoparticles illuminated by the tightly focused radially polarized beam

Nanoparticles	λ (nm)	Radius (nm)	K_r
Au in air	548	63	6.827
Au in glass	570	31	22.57
Ag in air	357	12	162.4
Ag in glass	403	1	1379.80

Further, let us quantitatively compare the average radial intensity enhancement obtained from three cases; Case A: Plane wave (**Chapter 2**), Case B: Tightly focused linearly polarized (**Chapter 3**), and Case C: Tightly focused radially polarized beam.

To make a detailed comparison for the average intensity enhancement observed and the effect on the LSPR peak wavelength in the three different illuminations, we plotted individual curves of Au and Ag nanoparticles for radii: *r=10 nm, 25 nm, 50 nm, 70 nm and 90 nm*. The average radial intensity for a particular radius is plotted on a vertical axis, and the horizontal axis represents the wavelength of the incident beam ranging from 300 nm to 900 nm. The results showing distinct comparisons for the interaction of monometallic nanoparticles with three different incident beams are presented in Fig. 4.5 to Fig. 4.8.

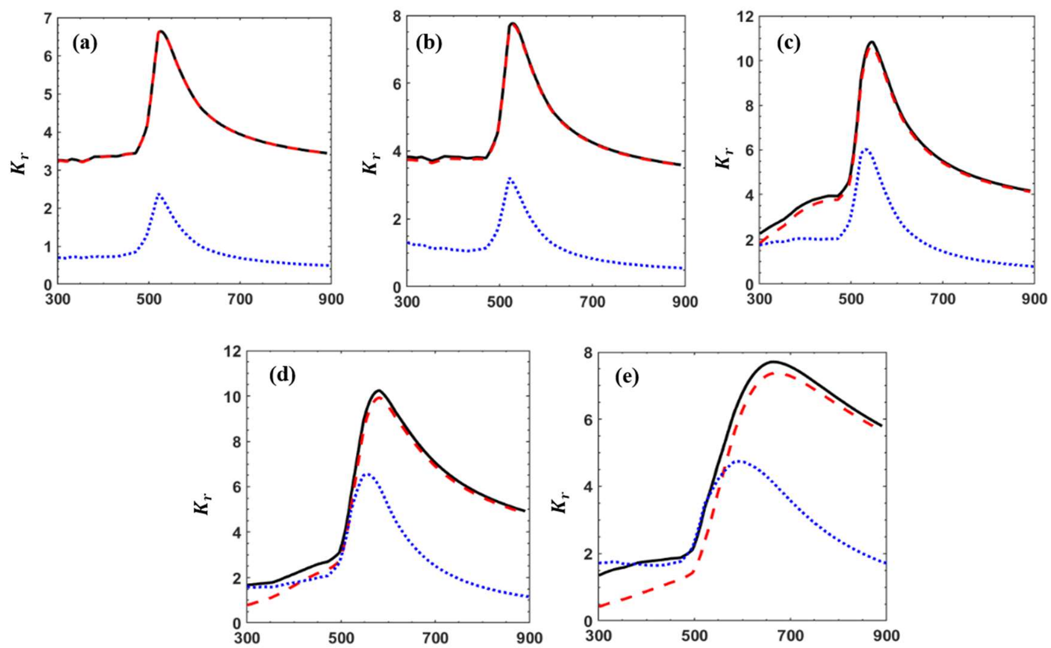

Fig. 4.5 Average radial intensity enhancement for an Au nanoparticle in air ($\boldsymbol{n_m = 1.00}$) illuminated by a linearly polarized plane wave (black); tightly focused linearly polarized beam (dashed red); tightly focused radially polarized beam (dotted blue). Particle size radius is (a) *r=10 nm,* (b) *r=25 nm,* (c) *r=50 nm,* (d) *r=70 nm, and* (e) *r=90 nm*.

The enhancement observed for a tightly focused linearly polarized beam is nearly the same as the enhancement observed for a plane wave. The maximum enhancement for an Au nanoparticle in dielectric media air is presented in Figs. 4.5 (a)-(e). The enhancement for case A and case B is the maximum for a smaller-size Au nanoparticle in glass as shown in Figs. 4.6 (a)-(c). The maximum enhancement is found in a tightly focused radially polarized incident beam in comparison to cases A and B for the size of nanoparticles greater than 55 nm in dielectric glass as shown in Figs. 4.6 (d), and (e).

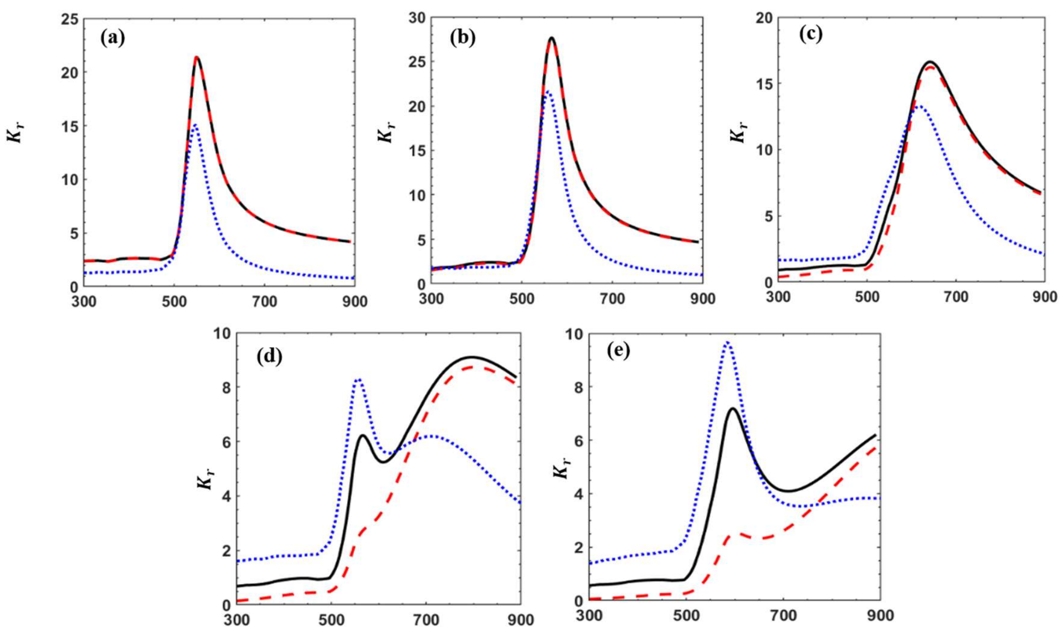

Fig. 4.6 Average radial intensity enhancement for an Au nanoparticle in glass ($\boldsymbol{n_m = 1.52}$) illuminated by a linearly polarized plane wave (black); tightly focused linearly polarized beam (dashed red); tightly focused radially polarized beam (dotted blue). Particle size radius is (a) *r=10 nm,* (b) *r=25 nm,* (c) *r=50 nm,* (d) *r=70 nm, and* (e) *r=90 nm*.

For a smaller Ag nanoparticle with a radius less than 50 nm, the results are nearly the same for the three illuminations and in both the dielectric media air and glass as shown in Figs. 4.7 (a), (b), and Figs. 4.8 (a), (b). The results presented in Figs. 4.7 (c)-(e) and Fig. 4.8 (c)-(e) show that the enhancement factor for a tightly focused radially polarized beam is the maximum in comparison to plane wave and tightly focused linearly polarized beam for a radius of the Ag nanoparticle beyond 30 nm. In the case of a radially polarized beam The spectrum is narrower for a radially polarized beam in comparison to a plane and tightly focused linearly polarized beam.

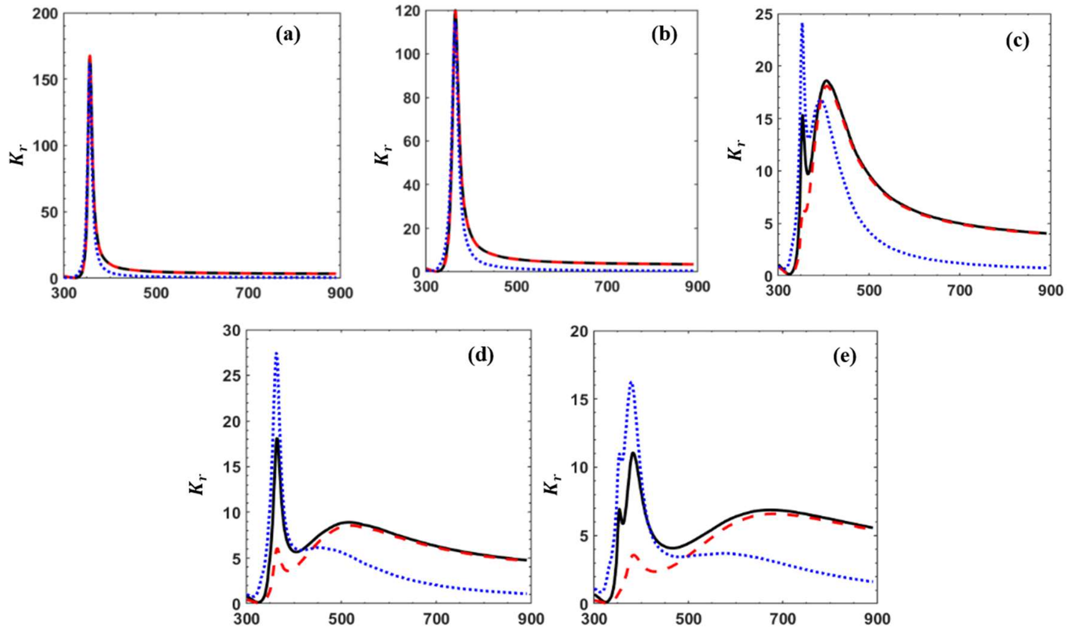

Fig. 4.7 Average radial intensity enhancement for an Ag nanoparticle in air ($\boldsymbol{n_m = 1.00}$) illuminated by a linearly polarized plane wave (black); tightly focused linearly polarized beam (dashed red); tightly focused radially polarized beam (dotted blue) , and the particle radius is (a) *r=10 nm,* (b) *r=25 nm,* (c) *r=50 nm,*(d) *r=70 nm, and* (e) *r=90 nm*.

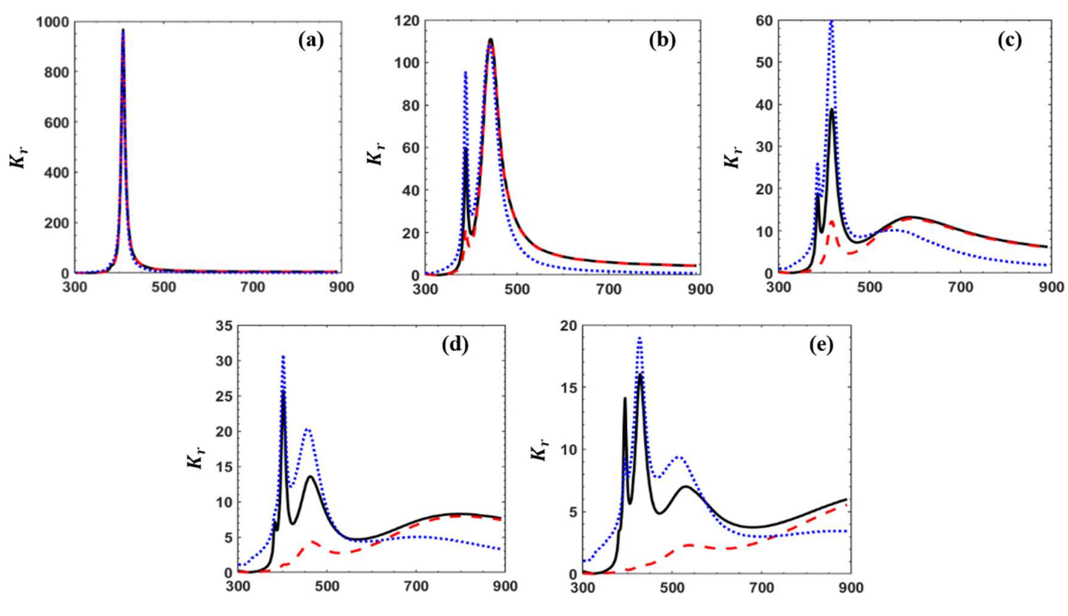

Fig. 4.8 Average radial intensity enhancement for an Ag nanoparticle in glass ($\boldsymbol{n_m = 1.52}$) illuminated by a linearly polarized plane wave (black); tightly focused linearly polarized beam (dashed red); tightly focused radially polarized beam (dotted blue), and the particle radius is (a) *r=10nm,* (b) *r=25nm,* (c) *r=50nm,*(d) *r=70nm, and* (e) *r=90nm*.

It is noted that the LSPR wavelength peak shifts towards a higher wavelength when the size of the nanoparticle is increased as shown in Fig. 4.5-4.8. The LSPR shifts from 527 nm to 664 nm wavelength in the air for an Au nanoparticle of varying radius 10 nm to 90 nm as shown in Fig. 4.5 (a), and Fig. 4.5 (e), whereas a shift from 550 nm to 596 nm is observed in the glass as shown in Fig. 4.6 (a), and Fig. 4.6 (e). For an Ag nanoparticle, the LSPR peak shifts from 357 nm to 379 nm wavelength in air, and from 409 nm to 429 nm wavelength in a glass medium for a nanoparticle of size ranging from 10 nm to 90 nm as shown in Figs. 4.7 (a), 4.7 (e), 4.8 (a), and 4.8 (e). Usually, a single LSPR peak is observed for an Au nanoparticle which shows the involvement of only a dipolar SPR ($n = 1$) as shown in Figs. 4.5 (a)-(e) and Figs. 4.6 (a)-(c). However, a larger size of an Au nanoparticle in glass generates more than one peak due to the involvement of the quadrupole ($n = 2$). In case of an Ag nanoparticle for both the dielectric media air and glass, dipolar ($n = 1$), quadrupole ($n = 2$) and higher no. of modes ($n = 3,4, \dots \infty$) are involved in the LSPR peak and hence generates multiple LSPR peaks when the size of nanoparticle is increased as shown in Figs. 4.7, and 4.8.

Since nanoparticles possessing plasmonic properties have direct application in the SERS, the average radial intensity enhancement is calculated at commonly used laser wavelengths in the Raman spectroscopy and results are shown in Table 4.2 and Table 4.3.

For observing the enhancement factor in the case of an Au nanoparticle the incident light wavelengths 532 nm, 633 nm, and 785 nm are selected. The spectrum of enhancement factor in the case of an Ag nanoparticle lies in the 350-450 nm wavelength region. We observed the average intensity enhancement for wavelengths 405 nm, 488 nm, and 532 nm. In addition to the laser wavelengths commonly used in Raman spectroscopy, maximum intensity enhancement can be observed at other wavelengths such as 557 nm and 584 nm for an Au nanoparticle in glass using a tightly focused radially polarized beam as shown in Figs. 4.6 (c), and (d). A maximum intensity enhancement in the case of scattering of a tightly focused radially polarized beam from an Ag nanoparticle is observed at wavelengths 353 nm, 363 nm, and 380 nm, in air as shown in Fig. 4.7 (c) –(e). On the other hand, in glass medium for wavelengths 388 nm, 402 nm, 416 nm, 428 nm maximum enhancement factor for an Ag nanoparticle is observed as shown in Fig. 4.8 (b-e). For achieving maximum intensity enhancement using a tightly focused radially polarized beam, a tunable laser wavelength source can be used.

Table 4.2. Maximum Enhancement factor observed for Au nanoparticle under different conditions at wavelengths used in SERS

Incident light	Incident Laser Wavelength											
	532 nm				633 nm				785 nm			
	Air		Glass		Air		Glass		Air		Glass	
	$\boldsymbol{a}$ (nm)	$\boldsymbol{K_r}$	$\boldsymbol{a}$ (nm)	$\boldsymbol{K_r}$	$\boldsymbol{a}$ (nm)	$\boldsymbol{K_r}$	$\boldsymbol{a}$ (nm)	$\boldsymbol{K_r}$	$\boldsymbol{a}$ (nm)	$\boldsymbol{K_r}$	$\boldsymbol{a}$ (nm)	$\boldsymbol{K_r}$
Case A: Plane wave	50	10.31	11	14.60	74	8.89	43	19.46	96	6.83	60	10.19
Case B: Tightly focused linearly polarized beam	49	10.11	11	14.56	74	8.64	43	19.16	94	6.60	60	9.92
Case C: Tightly focused radially polarized beam	58	6.48	18	13.03	84	4.64	46	13.50	100	2.88	67	5.61

Table 4.3. Maximum Enhancement factor observed for Ag nanoparticle under different conditions at wavelengths used in SERS

Incident light	Incident Laser Wavelength											
	405 nm				488 nm				532 nm			
	Air		Glass		Air		Glass		Air		Glass	
	$\boldsymbol{a}$ (nm)	$\boldsymbol{K_r}$	$\boldsymbol{a}$ (nm)	$\boldsymbol{K_r}$	$\boldsymbol{a}$ (nm)	$\boldsymbol{K_r}$	$\boldsymbol{a}$ (nm)	$\boldsymbol{K_r}$	$\boldsymbol{a}$ (nm))	$\boldsymbol{K_r}$	$\boldsymbol{a}$ (nm)	$\boldsymbol{K_r}$
Case A: Plane wave	41	25.24	5	1338	57	11.06	31	39.46	63	9.25	37	22.52
Case B: Tightly focused linearly polarized beam	41	24.93	5	1338	57	10.78	31	39.11	63	8.99	37	22.20
Case C: Tightly focused radially polarized beam	44	18.39	5	1329	63	6.29	32	31.14	71	4.86	39	15.94

4.3.2 Core-shell nanoparticles

Enhancement factors for a tightly focused radially polarized beam scattered through an uncoated Au, Ag nanoparticle, coated Ag@Au, and Au@Ag nanoparticle in different dielectric media are shown in Fig. 4.9 (a)-(d). A single LSPR peak is observed for an uncoated Au nanoparticle as shown in Fig. 4.9 (a) in air, and BK7. The maximum intensity enhancement is 2.837 at 521 nm wavelength in the air, whereas it becomes 19.52 at wavelength 551 nm in the BK7. On the other hand, two resonances are noticed with an enhancement factor of 127.6 for the first-order LSPR peak, and 64.26 for second-order LSPR at wavelengths 819 nm, and 711 nm respectively for an Au nanoparticle in the silicon. A single LSPR peak with an enhancement factor of 144.1 is observed at wavelength 361 nm for an uncoated Ag nanoparticle in air, whereas more than one resonance peaks are observed in BK7 and silicon as shown in Fig. 4.9 (b). The enhancement factor is 237.4 at wavelength 428 nm, and 74.86 at wavelength 387 nm corresponding to first-order, and second-order LSPR peaks respectively. The first-order LSPR peak in silicon medium is observed at wavelength 766 nm with an enhancement factor of 156.3. The enhancement factor 293.6 is observed for the second-order LSPR peak at wavelength 634 nm.

The enhancement factors for an Ag@Au nanoparticle in different media are presented in Fig. 4.9 (c). The maximum enhancement is 2.793 at wavelength 521 nm in air, and the enhancement factor becomes 19.44 at wavelength 549 nm in the BK7 medium. In silicon medium, the enhancement factor is 128.6 for the first-order LSPR peak at 818 nm wavelength, whereas the enhancement factor for the second-order LSPR peak becomes 64.76 at 710nm wavelength.

An enhancement factor of 88.05 is observed at wavelength 360 nm for a coated Au@Ag nanoparticle in the air as shown in Fig. 4.9 (d). In BK7, the first-order LSPR shows an enhancement factor of 152.2 at wavelength 429 nm, and the second-order LSPR peak is having an enhancement factor of 67.46 at wavelength 387 nm. In the silicon medium, the first-order LSPR peak is observed at 768 nm with an intensity enhancement of 156, and the second-order LSPR peak shows a maximum intensity enhancement of 291.5 at 634 nm.

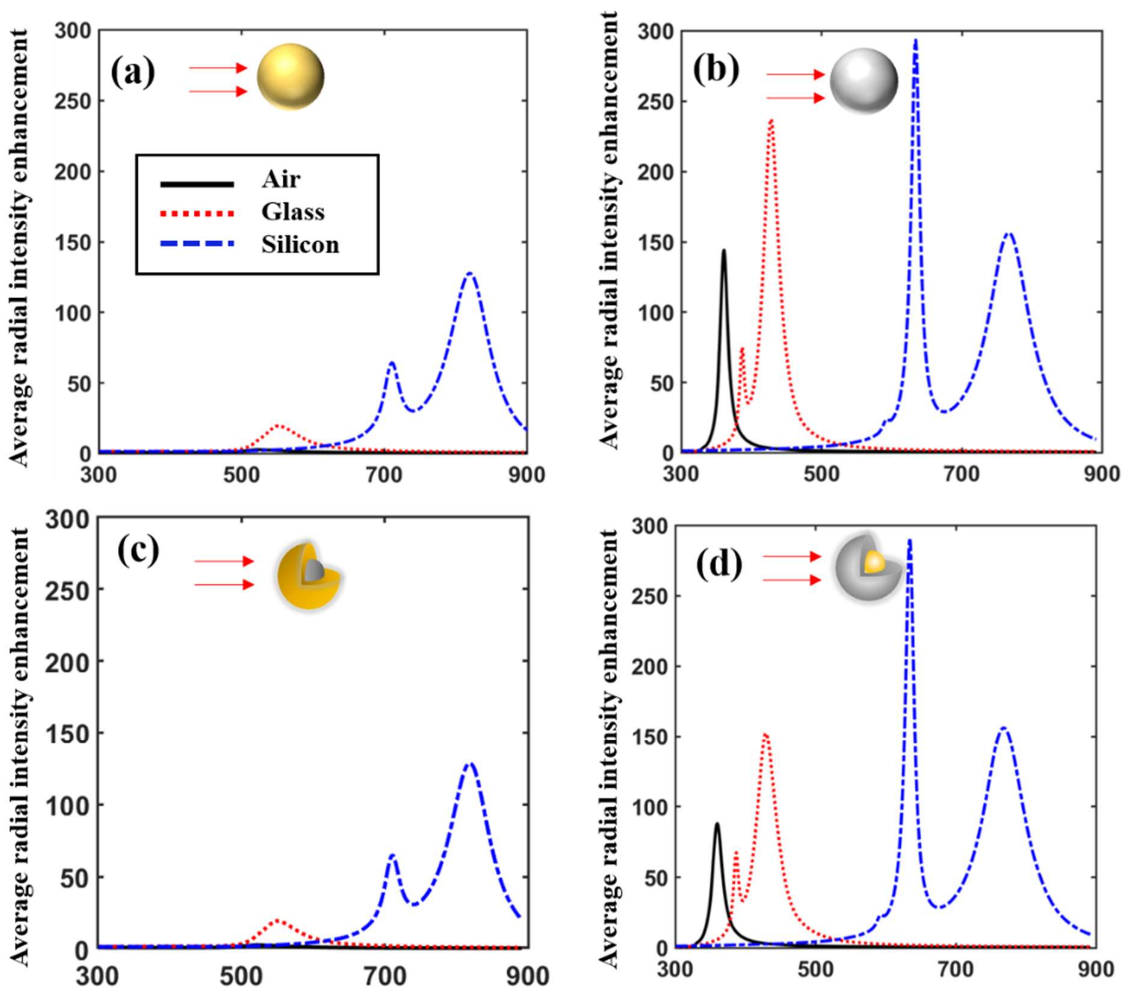

Fig. 4.9 Average radial intensity enhancement for an incident tightly focused radially polarized beam interacting with an (a) uncoated Au (b) uncoated Ag, (c) Ag@Au, and (d) Au@Ag nanoparticle in different dielectric media air (black), BK7 (glass) (··· red), and silicon (- – - blue).

It is observed that an uncoated Au nanoparticle, and coated Ag@Au nanoparticle show lesser intensity enhancement in comparison to an uncoated Ag nanoparticle, and coated Au@Ag nanoparticle. It is also observed that a coated Au@Ag nanoparticle is a highly suitable option for investigating the plasmonic properties under different illuminations in comparison to an

Ag@Au nanoparticle. An uncoated Ag nanoparticle shows significantly higher values of intensity enhancement in BK7. While illuminating an Ag nanoparticle from a tightly focused radially polarized beam in a silicon medium makes the intensity enhancement maximum in comparison to all the other cases. However, an Ag nanoparticle has the inherent issue of oxidation. Illumination of Au@Ag nanoparticle in silicon medium by a tightly focused radially polarized beam gives a maximum intensity enhancement as shown in Fig. 4.9 (d). The structure of the beam at focus changes when the polarization of the beam is changed from linear to radial, which affects the enhancement factor. Along with a higher enhancement factor, coated Au@Ag nanoparticle provides higher stability with reduced oxidization in different dielectric media and spherical symmetry. In Fig. 4.9, the red shift in the LSPR wavelength peak is observed with increasing refractive index of the surrounding dielectric media from air to silicon due to the fulfillment of resonance conditions at different wavelengths. Involvement of higher order multipoles is observed in silicon medium.

Now we compare the average radial intensity enhancement for three incident beams interacting with uncoated Au, uncoated Ag, core-shell Ag@Au, and Au @Ag nanoparticles, in different dielectric media. We have tabulated maximum intensity enhancement in Table 4.4 for three different cases; Case A: Plane wave (**Chapter 2**), Case B: Tightly focused linearly polarized (**Chapter 3**), and Case C: Tightly focused radially polarized beam.

On coating Au nanoparticle with an Ag metal layer, a shift in the LSPR towards lower wavelengths is also observed in Fig. 2.7 (**Chapter 2**), Fig. 3.10 (**Chapter 3**), and Fig. 4.9 which shows the effect of Ag coating.

Table 4.4. Maximum intensity enhancement for different nanoparticles under different illumination conditions

Nanoparticles	Dielectric medium	Case A: Plane wave		Case B: Tightly focused linearly polarized beam		Case C: Tightly focused radially polarized beam	
		K_r	λ (nm)	K_r	λ (nm)	K_r	λ (nm)
Uncoated Au	Air	7.28	527	7.25	527	2.84	521
	BK7 (glass)	25.62	558	25.49	558	19.52	551
	Silicon	130.40	823	130.00	823	127.60	820
Uncoated Ag	Air	149.50	361	149.20	361	144.10	361
	BK7 (glass)	241.30	429	240.9	429	237.40	428
	Silicon	188.90	634	159.20	770	293.60	634
Core-shell Ag@Au	Air	7.252	525	7.22	526	2.79	521
	BK7 (glass)	25.51	556	25.38	556	19.44	549
	Silicon	131.30	822	130.90	822	128.60	818
Core-shell Au@Ag	Air	93.13	361	92.85	361	88.05	360
	BK7 (glass)	156.00	430	155.60	430	152.20	429
	Silicon	187.30	634	158.90	771	291.5	634

Scattering of a tightly focused radially polarized beam from an Au@Ag core-shell nanoparticle of variable shell thickness is investigated for incident beam wavelength ranging from 300 nm to 900 nm. We kept the inner Au core fixed ($a = 6\ nm$), and the overall radius within a range of $b = 10\ nm$ to $b = 100\ nm$. Changes in average radial intensity enhancement with varying outer shell thickness in different dielectric media air, BK7 (glass), and silicon are highlighted in Fig. 4.10. The color bar represents the average radial intensity enhancement.

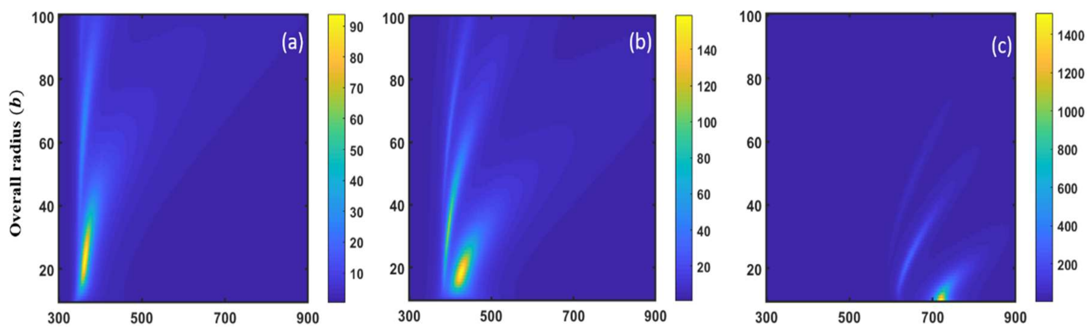

Fig. 4.10 Average radial intensity enhancement for an incident tightly focused radially polarized beam interacting with an Au@Ag nanoparticle of variable overall radius ranging from 20 nm to 100 nm and in different dielectric media (a) air (b) BK7 (glass), and (c) silicon.

To further understand the variation in intensity enhancement due to increasing Ag shell thickness, a detailed investigation is carried out for the overall radius $b = 40\ nm, 60\ nm, 80\ nm$ as presented in Table 4.5. The data points are manually noted for the maximum intensity enhancement at the respective overall radius and wavelength from our numerical results on the MATLAB platform. The LSPR peak shows a maximum enhancement factor for the corresponding overall radius 'b' are presented in Table 4.5.

Table 4.5. Maximum Enhancement factor for a varying Ag shell thickness of an Au@Ag core-shell nanoparticle (Au core radius $a = 6\ nm$) under a tightly focused radially polarized beam illumination

Overall radius, b (nm)	Air	BK7 (glass)	Silicon
40	35.90 (379 nm)	98.78 (403 nm)	89.92 (714 nm)
60	28.23 (357 nm)	34.84 (436 nm)	44.48 (694 nm)
80	22.23 (370 nm)	24.53 (415 nm)	18.11 (767 nm)

Based on the results obtained for Case A: Plane wave (Table 2.3, **Chapter 2**), Case B: Tightly focused linearly polarized (Table 3.2, **Chapter 3**), and Case C: Tightly focused radially polarized beam, we discussed the change in average intensity enhancement for varying outer shell thickness.

The enhancement factor is 62.84 at wavelength 403 nm for a coated nanoparticle of overall radius $b = 40\ nm$ illuminated with a plane wave. This further increased to 98.78 for a tightly focused radially polarized beam in the BK7 medium. An increase in the enhancement factor with an increase in the Ag shell thickness is observed for a tightly focused radially polarized beam in the BK7 and silicon medium. A maximum intensity enhancement is noticed for the scattering of a tightly focused radially polarized beam by an Au@Ag nanoparticle for overall radius $b = 60\ nm$ in all the dielectric media as shown in Table 4.5. From Table 4.5, one can find an optimum thickness for an Au@Ag nanoparticle for a particular wavelength of the incident beam. With increase in thickness of the Ag shell in the Au@Ag nanoparticle, the

LSPR peak wavelength shifts closer to the LSPR peak observed for an Ag nanoparticle due to an increase in size of the particle.

Average radial intensity enhancement due to the plasmonic response of Au@Ag nanoparticle with varying outer shell thickness are presented in Fig. 2.8 (**Chapter 2**), Fig. 3.11 (**Chapter 3**), and Fig. 4.10 for three different illuminations, and Table 4.6 highlights the maximum enhancements factors for Au@Ag core-shell nanoparticle under different conditions.

Table 4.6. Maximum Enhancement factor observed for Au@Ag core-shell nanoparticle under different conditions

Dielectric medium	Case A: Plane wave			Case B: Tightly focused linearly polarized beam			Case C: Tightly focused radially polarized beam		
	λ (nm)	b (nm)	K_r	λ (nm)	b (nm)	K_r	λ (nm)	b (nm)	K_r
Air	363	23	98.84	363	23	98.51	362	23	93.85
BK7 (glass)	426	18	163.3	426	18	162.9	425	18	159.1
Silicon	721	10	1519	721	10	1519	721	10	1512

Table 4.6 suggests that an Au core radius of 6 nm and an overall radius of 20 nm for an Au@Ag nanoparticle show similar values of maximum intensity enhancement factor for all three different illuminations. It is observed that for an Au@Ag coated nanoparticle with a core radius $a = 6\ nm,$ the optimum thickness of Ag shell is 17 nm, 12 nm, and 4 nm in air, BK7, and silicon medium respectively as presented in Table 4.6. The intensity enhancement is maximum for a silicon medium under all three illuminations.

4.4 Conclusion

This chapter presents results on Mie scattering of a tightly focused radially polarized beam for wavelength ranging from 300 nm to 900 nm. The scattering is considered in different dielectric media using a multipole expansion formalism. The influence of the polarization state of a tightly focused beam on the plasmonic response of a nanoparticle is examined and discussed. Near-field intensity enhancement on the surface of a nanoparticle is affected by the polarization distribution of the incident beam and this is demonstrated by developing a Mie Scattering Algorithm on the MATLAB platform. The radial component of average intensity shows a significant contribution in the near-field enhancement, and the results are presented for monometallic Au, Ag nanoparticles and Ag@Au, Au@Ag core-shell nanoparticles. An intensity enhancement factor is also evaluated for the scattering of a tightly focused radially polarized beam from the core-shell nanoparticles of fixed core and variable outer shell thickness. A comparison of the average radial intensity enhancements for three different incident beams namely plane wave, tightly focused linearly polarized, and tightly focused radially polarized incident beam is presented.